A Comparative Study of the Electrooxidation of Ethylene Glycol on Transition Metal Electrodes in Alkaline Solution

I. Danaee[*,1], M. Jafarian[2], A.A. Shahnazi Sangachin[1] and F. Gobal[3]

[1]Abadan Faculty of Petroleum Engineering, Petroleum University of Technology, Abadan, Iran
[2]Departement of chemistry, K. N. Toosi University of Technology, Tehran, Iran
[3]Departement of chemistry, Sharif University of Technology, Tehran, Iran

Abstract: *Electrodes made of group VIII and IB metals were examined for their redox process and electrocatalytic activities towards the oxidation of ethylene glycol in alkaline solutions. The method of cyclic voltammetery (CV) and Open circuit potentials measurement (OCP) was employed. It is found that considerable electrooxidation current are observed for silver and copper but lower anodic overpotential for oxidation is obtained for gold and platinum. Oxide layer produced on the surface of all electrodes in alkaline solution under anodic scan participates in ethylene glycol electrooxidation. Oxidation current observed in the reverse scans for platinum and gold are higher than those observed in forward potential scan. Open circuit potential measurements have shown the interaction of ethylene glycol and electrodes.*

Keywords: Transition metal; Electrooxidation; Ethylene glycol; Open circuit.

1. INTRODUCTION

Alkaline membrane fuel cell can be a good alternative to proton exchange membrane fuel cell (PEMFC). The oxidation and reduction reactions occurring in fuel cells are more facile in alkaline media [1,2] than in acid solution. The crossover of fuel is avoided due to the transfer of hydroxyl groups from the cathode side to the anode side by electro-osmosis. In fuel cell systems, the use of hydrogen is limited by the problems of production, purification, storage and distribution. Then, liquid fuels can be of interest.

So far methanol has been considered to be the best fuel [3]. However, the use of methanol as a fuel presents several problems: methanol is toxic; it is highly flammable, has a low boiling point (65 °C) and is highly prone to pass through the polymer electrolyte membrane (high crossover). Fuel crossover lowers the operating potential of the oxygen electrode and results in the consumption of fuel and generation of heat without the production of useful electrical energy. It is obviously desirable to minimize the rate of fuel crossover. However, the works of the Petrii group [4] about the behavior of alcohols containing more than one carbon atom pointed out that a low faradic efficiency was generally encoun-

tered in fuel cell due to the difficulty to break the C–C bond at low temperature. Recent works showed that the reaction products detected in the anode outlet of a direct ethanol fuel cell (DEFC) were acetic acid, acetaldehyde and CO_2 [5]. It seems that only the carbon carrying the oxygen species is oxidized, since CH_4 was also detected in ethanol electrooxidation at platinum based catalysts [6].

The electrooxidation of ethylene glycol (EG) has attracted considerable interest in recent years, both from practical reasons and from a fundamental point of view. Because of its higher energy density, lower toxicity, lower flammability, and lower permeation through the polymer electrolyte membrane compared to methanol, EG has been considered as an attractive for Direct Alcohol Fuel Cell (DAFC) applications [7,8]. The successful introduction of a DAFC based on EG oxidation is hindered, however, by the slow kinetics of the EG electrooxidation reaction and by its tendency to mainly produce incomplete oxidation products rather than the complete oxidation to CO_2 [9,10].

The observation of a large variety of incomplete oxidation products (glycolaldehyde, glyoxal, glycolic acid, glyoxylic acid and oxalic acid), which were detected by in situ infrared spectroscopy [11,12] or by chromatographic product analysis [13,14] on the one hand and of strongly adsorbed or soluble C1 species such as CO_{ad}

*To whom correspondence should be addressed: Email: danaee@put.ac.ir
Phone: (0098631) 4429937

[15,16] formic acid, and formaldehyde [14] on the other hand, led to the conclusion that EG oxidation can proceed *via* two different pathways. The first pathway involves C–C bond breaking and subsequent oxidation of the C1 fragments. Alternatively the reaction proceeds *via* sequential oxidation of the functional groups without attacking the C–C bond with the final product being oxalic acid.

Fleischmann et al [17] proposed long ago that the rate determining step in the electrooxidation of many organic compounds on Ni was a chemical reaction in which NiOOH abstracted a hydrogen atom from the adsorbed species, according to the reaction (in the case of primary alcohols).

$$RCH_2OH_{ads} + NiOOH \rightarrow RC^{\cdot}HOH + Ni(OH)_2 \qquad (1)$$

In this way they could rationalize that although there was a current plateau, its current was not increased by stirring, since it was proportional to the alcohol coverage. This model also applies, at least partly, to Pt, since it has been shown by EQCM [18] that both a loss of mass and an anodic current are observed when *n*-hexanol is added to the electrolyte.

In fact, the choice of a suitable electrode material is an important factor that may affect the performance of electrocatalysts owing to interactions and surface reactivity [19-20]. Nickel and copper have been used as electrocatalyst due to low cost only in alkaline solution. On the other hand, Pt and Au have been applicable in both basic and acidic solution.

The present work investigates the effect of the nature of the electrode catalysts on ethylene glycol electrooxidation. Different material such as Pt, Au, Ag, Ni and Cu are used as working electrodes in alkaline solution. The study of ethylene glycol oxidation on different electrode may provide valuable data for development of high active catalysts for electrooxidation in alkaline medium.

2. EXPERIMENTAL

Sodium hydroxide and ethylene glycol used in this work were Merck product of analytical grade and were used without further purification. Doubly distilled water was used throughout. Electrochemical studies were carried out in a conventional three electrode cell powered by an electrochemical system comprising of EG&G model 273 potentiostat/galvanostat. The system is run by a PC through M270 commercial software via a GPIB interface. Open circuit potential measurements were performed by a potentiostat/galvanostat Solarton model 1266. A dual Ag/AgCl-Saturated KCl, a graphite rode and a metal disk electrode were used as the reference, counter and working electrodes, respectively.

Samples for electrochemical experiments were cut from a cylindrical rod with a cutter machine. Each sample sealed by polyester resin so the exposed surface area of each electrode is equal to 0.0314 cm^2. The working electrode was polished with 0.05 mm alumina powder on a polishing microcloth and rinsed thoroughly with doubly distilled water. Voltametric experiments were done in a beaker containing 200 ml of 0.1 M NaOH solution at the temperature of 25±2 °C. Experiments were carried out from cathodic to anodic potential limit with scan rate 20 mV s^{-1}.

3. RESULTS AND DISCUSSIONS

Figure 1 shows the cyclic voltammograms of Pt electrode without and with 0.2 M ethylene glycol in 0.1 M NaOH solution. In the
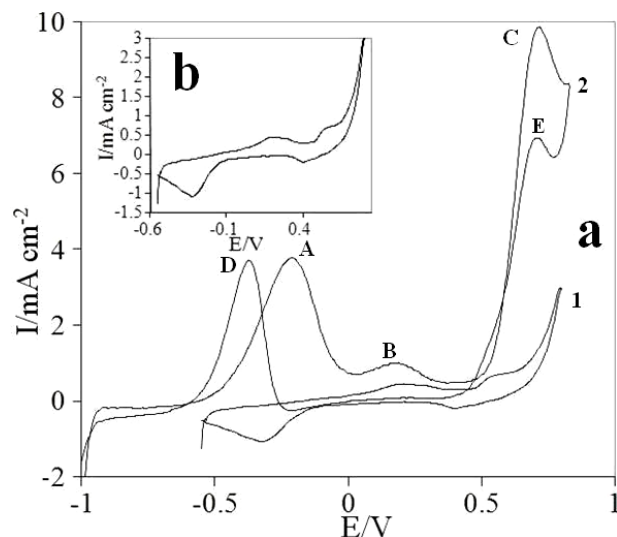

Figure 1. (a) Cyclic voltammograms of platinum electrode in 0.1 M NaOH solution in absence (1) and presence (2) of 0.2 M ethylene glycol at a scan rate of 20 mV s^{-1}. (b) Cyclic voltammogram of platinum electrode in 0.1 M NaOH solution.

absence of ethylene glycol, two oxidation peaks observed in anodic scan and two reductions observed in cathodic scan. Oxidation peaks at the potentials of 230 and 570 mV in anodic half cycle are due to the adsorption of Pt oxide/hydroxides and well defined cathodic peaks were attributed to the reduction of the oxide/hydrous oxide layer. The formation of Pt oxide corresponds to a two step reaction mechanism that takes place with PtOH as intermediate, according to the following reactions [21]:

$$Pt + OH^- \rightarrow PtOH + e \qquad (2)$$

$$Pt + OH \rightarrow PtO + H^+ + e \qquad (3)$$

The first step of Pt oxidation occurs reversibly when the surface is almost completely covered with a monolayer of hydroxides [21]. The PtOH formed may also participate in a place-exchange mechanism to form HOPt [22,23]. This oxide formation is believed to cause or enhance the catalytic properties of inert metals. It has also been reported that the reduction of oxides gradually becomes irreversible [24]. However, the reaction mechanism appears to be very complex. In anodic scan, the current density was negative up to -0.3 V which was due to the reduction of the oxide layer that was remained or produced on electrode surface after polishing.

Three oxidation peaks (A, B and C) appeared in the anodic half cycle in the presence of 0.2 M ethylene glycol while peaks E and D, still anodic, appear in the ensued cathodic half cycle. Ethylene glycol is adsorbed preferentially on the electrode surface in this potential region and inhibits hydrogen adsorption on the electrode surface. The current density of peak A is proportional to potential sweep rates (dV/dt) while the current density of peak C is proportional to the square root of sweep rates. Thus, peak C apparently represents a diffusion controlled process. No familiar quantitative relation between the peak B current density and dV/dt seems to exit. However, the linear relation between the peak current density
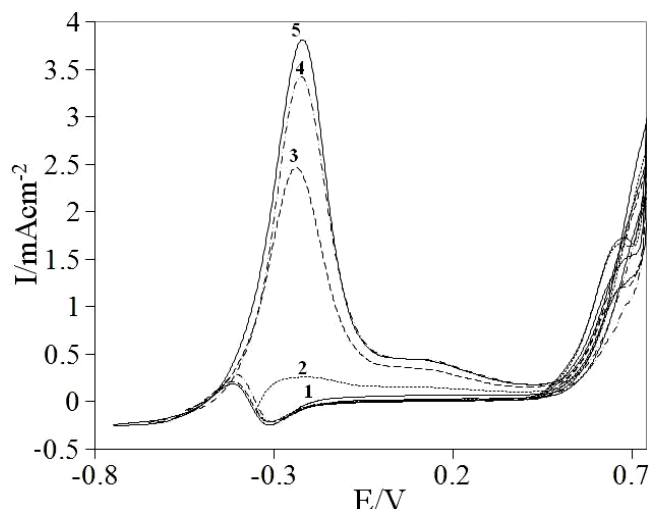
Figure 2. The effect of the lower limiting potential on 0.2 M ethylene glycol oxidation at Pt electrode with scanning from 0.73 V in 0.1 M NaOH at a scan rate of 20 mV s^{-1}.
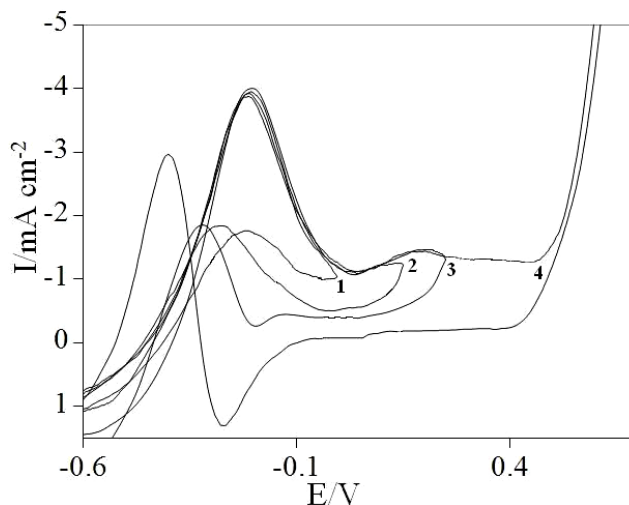

Figure 3. The effect of the upper limiting potential on 0.2 M ethylene glycol oxidation at Pt electrode with scanning from -0.6 V in 0.1 M NaOH at a scan rate of 20 mV s^{-1}.

of A and the scan rate indicates that the process A has the characteristics of the surface processes of an adsorbed species.

The first oxidation peak, A, may be attributed to the oxidative dehydrogenation of ethylene glycol at the platinum surface. The first step in ethylene glycol oxidation should be the ethylene glycol adsorption:

$$CH_2(OH)CH_2(OH) \rightarrow [CH_2(OH)CH_2(OH)]_{ads} \quad (4)$$
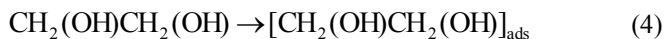
Hughes et al [25] and Skou [26] reported similar experimental phenomena, but using conventional voltammetry. EG$_{ads}$ of previous step decomposes further as follows [27]:
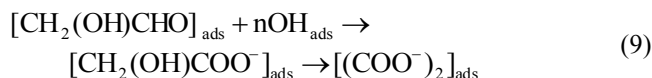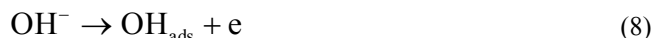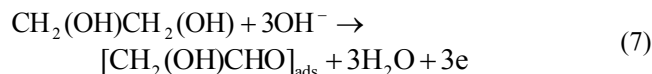
$$[CH_2(OH)CH_2(OH)]_{ads} \rightarrow [CH_2(OH)CH(OH)]_{ads} + H_{ads} \quad (5)$$

The adsorbed hydrogen atom is in equilibrium with H$^+$ and the electron:

$$H_{ads} \rightarrow H^+ + e \quad (6)$$

The effect of the lower limiting potential with scanning from 0.73 V vs. Ag/AgCl is shown in figure 2. As can be seen, in the low potential range only peak C appears. When the potential cycle is limited in the region positive of -350 mV, we do not observe peak B. With decreasing lower potential limit to the negative of potential of peak A, then peak B is produced. Clearly, process A has an effect on process B. This means that peak B is due to further oxidation of the adsorbed intermediates produced in process A. However, peak C remained almost independent of peaks A and B. It seems that it corresponds to the direct oxidation of ethylene glycol from the bulk or probably due to the reaction of PtOH and PtO with ethylene glycol diffused in the bulk. Oxidation of ethylene glycol occurs not only in the anodic but also continues in the initial stage of the cathodic half cycle, peak E. The onsets potential for ethylene glycol oxidation coincides with the completion of OH$^-$ anion adsorption, therefore the oxide species probably take part in
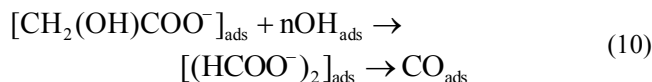
the ethylene glycol oxidation.

In the light of our results and the literature data [28-30], we discuss the reaction scheme of ethylene glycol oxidation on Pt surface as follows. A dual path mechanism for oxidation on a Pt surface in alkaline media is suggested. No poisoning path oxalate COO$^-$ is produced as follows:

$$CH_2(OH)CH_2(OH) + 3OH^- \rightarrow [CH_2(OH)CHO]_{ads} + 3H_2O + 3e \quad (7)$$

$$OH^- \rightarrow OH_{ads} + e \quad (8)$$

$$[CH_2(OH)CHO]_{ads} + nOH_{ads} \rightarrow [CH_2(OH)COO^-]_{ads} \rightarrow [(COO^-)_2]_{ads} \quad (9)$$

Also adsorbed species such as (CHO)2 and CHOCOO- could be participated as intermediates in oxidation reaction [28-30].

In poisoning path the C-C bond of glycolate CH$_2$(OH)COO$^-$ and glyoxal (CHO)$_2$ break to formate HCOO$^-$ production and therefore poisoning species CO$_{ads}$ is produced:

$$[CH_2(OH)COO^-]_{ads} + nOH_{ads} \rightarrow [(HCOO^-)_2]_{ads} \rightarrow CO_{ads} \quad (10)$$

Matsuoka et al [31] reported electrooxidation of ethylene glycol and methanol on platinum electrode in alkaline solution by current transient studies. Ethylene glycol showed much less significant electrode poisoning than methanol at low applied anodic potential. This phenomenon was clarified by analyzing the products of ethylene glycol oxidation where oxalate and glycolate was obtained as the main product. In higher applied potential, formate is produced as the main product and therefore the poisoning of the surface occurs.

Figure 3 shows the effect of the upper limiting potential on peak D with scanning from -0.6 V. When the upper limit of potential is
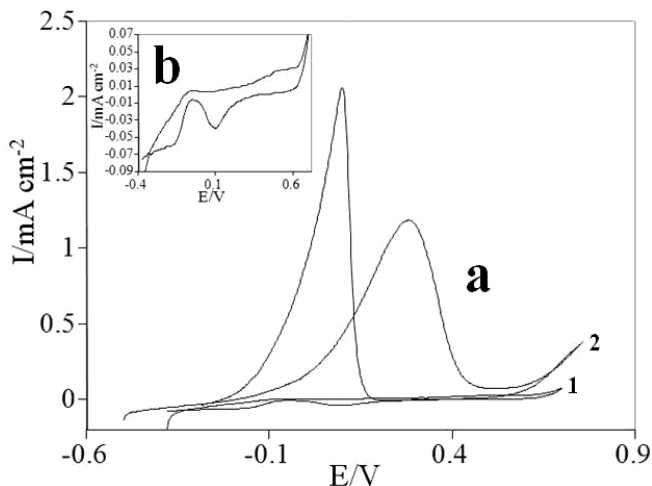
Figure 4. (a) Cyclic voltammograms of gold electrode in 0.1 M NaOH solution in absence (1) and presence (2) of 0.2 M ethylene glycol at a scan rate of 20 mV s^{-1}. (b) Cyclic voltammogram of gold electrode in 0.1 M NaOH solution.

Figure 5. (a) Cyclic voltammograms in the absence (1) and the presence of 0.1 M of (2) ethylene glycon on Ni electrode in 0.1 M NaOH solution. Potential sweep rate was 20 mV s^{-1}. (b) Initial potential of ethylene glycol oxidation.

lower than 0 V, peak D appears in the same potential of peak A. With increasing upper limiting potential, peak D shift to more negative potential position. It seems that the oxide produced at higher potentials should be reduced before the processes D. Therefore oxidation in low applied potential occurred with some delay. Also, increasing current in peak D was observed with increasing upper limit of potential suggesting that the poison partly covers the surface and is removed in higher anodic potential.

The set of cyclic voltammograms presented in Figure 4 illustrate the electrooxidation activities of 0.2 M ethylene glycol at gold in alkaline medium. For the sake of comparison, the cyclic voltammogram of the bare electrode in the supporting electrolyte, 0.1 M NaOH, under the same experimental condition is included Fig. 4b. In alkaline supporting electrolyte, the curve displays increasing current from 250 mV and a broad peak at 540 mV, has a reduction current peak appearing near 90 mV on its negative side. The increasing current is due to OH$^-$ adsorption on Au surface to form short-lived AuOH species that is subsequently converted to surface oxide [32]. The broad anodic peak is associated with a surface oxidation process, and the cathodic peak corresponds to the reduction of the gold oxide formed in the anodic scan.

The ethylene glycol oxidation on gold electrode proceeds irreversibly in the potential range in which coadsorption of organic molecules and OH$^-$ ions occur. This suggests that the hydroxyl ions play an important role in the mechanism.

The oxidation of ethylene glycol starts in the positive sweep above -200 mV, Figure 4. As the electrode potential becomes increasingly positive, well defined anodic peak with maxima at 280 mV appear on the cyclic voltammograms but no corresponding reductive peak is found during the subsequent cathodic scan. In the negative going sweep, oxidation resumes when the surface oxide layer begins to reduce reaching a maximum at 96 mV versus Ag/AgCl. Reaction pathway in oxidation of ethylene glycol on gold electrode can be assumed in this case:
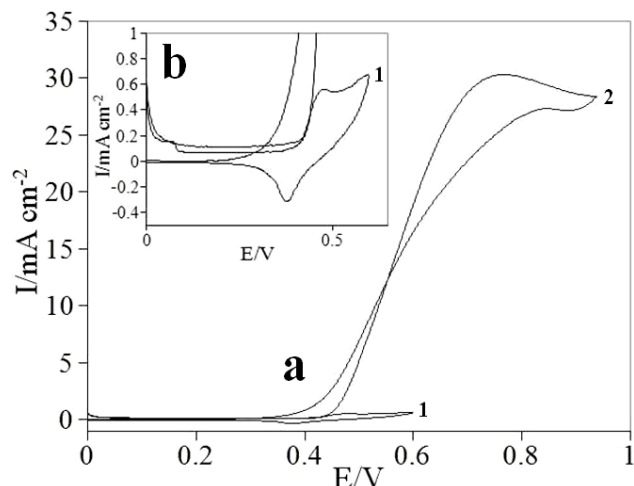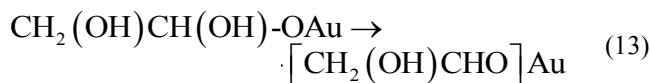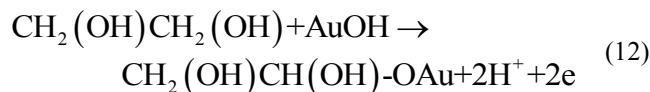
$$Au + OH^- \rightarrow AuOH + e \qquad (11)$$

$$CH_2(OH)CH_2(OH) + AuOH \rightarrow \\ CH_2(OH)CH(OH)\text{-}OAu + 2H^+ + 2e \qquad (12)$$

$$CH_2(OH)CH(OH)\text{-}OAu \rightarrow \\ \cdot\big[CH_2(OH)CHO\big]Au \qquad (13)$$

Parpot et al [33] reported with chromatographic analyses that electrooxidation of vicinal diols on gold surface with OH coverage lead to C-C rupture in following pathway:
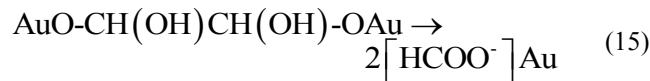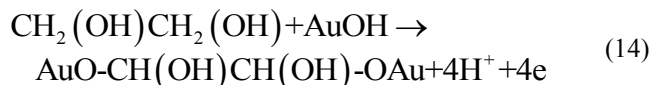
$$CH_2(OH)CH_2(OH) + AuOH \rightarrow \\ AuO\text{-}CH(OH)CH(OH)\text{-}OAu + 4H^+ + 4e \qquad (14)$$

$$AuO\text{-}CH(OH)CH(OH)\text{-}OAu \rightarrow \\ 2\big[HCOO^-\big]Au \qquad (15)$$

Figure 5 presents cyclic voltammograms of a Ni electrode in 0.1 M NaOH solution recorded at a potential sweep rate of 20 mV s^{-1}. A pair of redox peaks that appear at 480 and 375 mV vs. Ag/AgCl are assigned to Ni^{2+}/ Ni^{3+} redox couple in alkaline media [34].

Cyclic voltammograms of Ni electrode in 0.1 M NaOH solution in the presence of 0.2 M ethylene glycol at a potential sweep rate of 20 mV s^{-1} is presented in Fig. 5a. Oxidation of ethylene glycol appears as a typical electrocatalytic response. The anodic charge increased with respect to that observed in the absence of ethylene glycol and it was followed by decreasing the cathodic charge. So, catalytic electrooxidation of ethylene glycol on Ni seems to be certain.

The decreased cathodic current that was ensued the oxidation process in the reverse cycle indicates that the rate determining step

A Comparative Study of the Electrooxidation of Ethylene Glycol on Transition Metal Electrodes in Alkaline Solution / J. New Mat. Electrochem. Systems
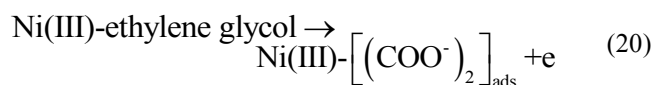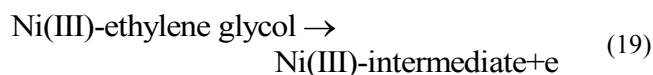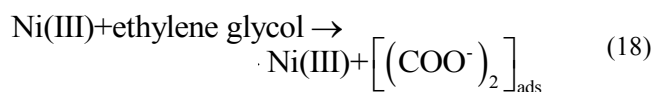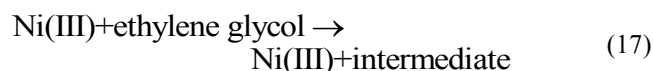
259

certainly involves ethylene glycol and that it is incapable of reducing the entire high valent nickel species formed in the oxidation cycle. The electrocatalytic oxidation of ethylene glycol occurs not only in the anodic but also continues in the initial stage of the cathodic half cycle. Ethylene glycol molecules adsorbed on the surface are oxidized at higher potentials parallel to the oxidation of Ni(II) to Ni(III) species. The later process has the consequence of decreasing the number of sites for ethylene glycol adsorption that along with the poisoning effect of the products or intermediates of the reaction tends to decrease the overall rate of ethylene glycol oxidation. Thus, the anodic current passes through a maximum as the potential is anodically swept. In the reverse half cycle, the oxidation continues and its corresponding current goes through the maximum due to the regeneration of active sites for adsorption of ethylene glycol as a result of the removal of adsorbed intermediates and products. Surely, the rate of ethylene glycol oxidation as signified by the anodic current in the cathodic half cycle drops as the unfavorable cathodic potentials are approached.

According to the high current density in presence of ethylene glycol and also observation of a new oxidation peak at 770 mV for ethylene glycol oxidation at a potential much more positive than that of the oxidation of $Ni(OH)_2$ potential we assume that part of the anodic current is due to ethylene glycol oxidation by NiOOH due to the disappearance of the NiOOH reduction peak in the negative sweep and part of the current is due to ethylene glycol oxidation on the surface of oxide layer by direct electro-oxidation [34].

The redox transition of nickel species present in the film is

$$Ni(II) \rightarrow Ni(III) + e^- \qquad (16)$$

and alcohols are oxidized on the modified surface via the following reaction

$$Ni(III) + \text{ethylene glycol} \rightarrow Ni(III) + \text{intermediate} \qquad (17)$$

$$Ni(III) + \text{ethylene glycol} \rightarrow Ni(III) + \left[\left(COO^- \right)_2 \right]_{ads} \qquad (18)$$

$$Ni(III) - \text{ethylene glycol} \rightarrow Ni(III) - \text{intermediate} + e \qquad (19)$$

$$Ni(III) - \text{ethylene glycol} \rightarrow Ni(III) - \left[\left(COO^- \right)_2 \right]_{ads} + e \qquad (20)$$

Eqs. (17) & (18) are according to Fleischmann mechanism and in Eqs. (19) & (20), Ni^{3+} used as active surface for ethylene glycol oxidation. Observation of a new oxidation peak for ethylene glycol oxidation at a potential much more positive than that of the oxidation of $Ni(OH)_2$ potential is according to Eqs. (19) & (20) [35,36].

Typical cyclic voltammogram of copper in 0.1 M NaOH solution and in the potential range of -650 to 850 mV is shown in Figure 6a where potential sweep rate of 20 mV s^{-1} has been employed. A number of well-defined peaks are observed in both the anodic and cathodic half cycles. Peak A1 has been attributed to oxygen adsorption based on the CV and in situ ellipsometric studies [37,38]. Peak A2 is due to the Cu/Cu(I) redox couple. At the working pH,
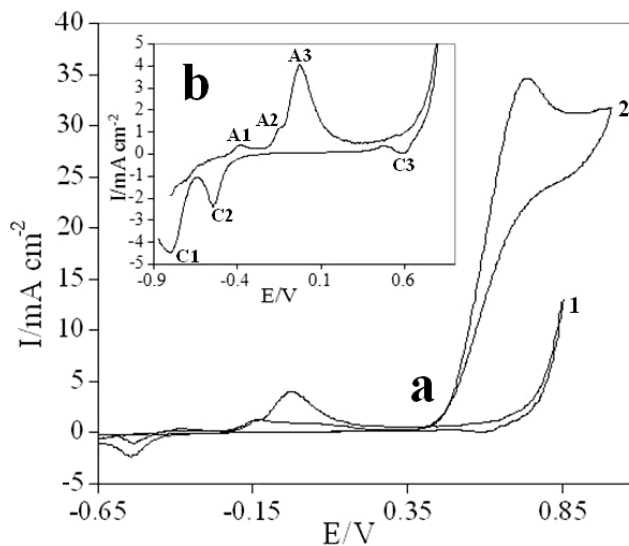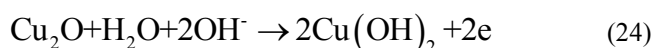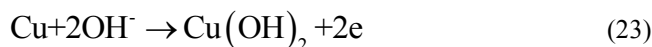

Figure 6. (a) Cyclic voltammograms of copper electrode in 0.1 M NaOH solution. (b) Typical cyclic voltammograms of copper electrode in 0.1 M NaOH solution in the absence (1) and presence (2) of 0.2 M ethylene glycol. (b) Cyclic voltammograms of copper electrode in 0.1 M NaOH solution. Potential sweep rate is 20 mV s^{-1}.

Cu(I)hydroxide is the main product which is transformed to the corresponding oxide upon aging [39] according to the following reactions:

$$Cu + OH^- \rightarrow CuOH + e \qquad (21)$$

$$2CuOH \rightarrow Cu_2O + H_2O \qquad (22)$$

Peak A3 is assigned to Cu to Cu(II) as well as Cu(I) to Cu(II) conversions through the following electrode processes [40]:

$$Cu + 2OH^- \rightarrow Cu\left(OH\right)_2 + 2e \qquad (23)$$

$$Cu_2O + H_2O + 2OH^- \rightarrow 2Cu\left(OH\right)_2 + 2e \qquad (24)$$

$$Cu\left(OH\right)_2 \rightarrow CuO + H_2O \qquad (25)$$

It has been reported [41] that beyond the peak A3 the formation of soluble species occurs, as proposed from cyclic chronopotentiometric studies [42]. Such soluble species are formed through:
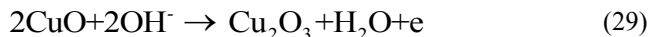
$$Cu + 3OH^- \rightarrow HCuO_2^- + H_2O + 2e \qquad (26)$$

and the dissolution equilibrium

$$Cu\left(OH\right)_2 + 2OH^- \rightarrow CuO_2^{2-} + 2H_2O \qquad (27)$$

The reactions to form Cu(III) during the anodic scan are postulated to be [39].

$$Cu\left(OH\right)_2 + 2OH^- \rightarrow CuO_2^- + 2H_2O + e \qquad (28)$$

and/or

$$2CuO + 2OH^- \rightarrow Cu_2O_3 + H_2O + e \quad (29)$$

It has been proposed that Cu(III) species are more easily formed, and indeed detected, at high hydroxide concentration [40]. In the present study, the oxidative wave for the formation of Cu(III) species may be under the rising current at about 700 mV. Similar observation has previously been reported by Miller [43] in a ring-disk voltammetric study of copper electrodes in alkaline solutions.

One small and two large reduction peaks were observed during the cathodic scan. These are assigned to the reduction of Cu(III) to Cu(II), peak C3, the reduction of Cu(II) to Cu(I), peak C2, and finally, the reduction of Cu(I) to Cu , peak C1.

Cyclic voltammogram of copper electrode in the presence of ethylene glycol at 0.2 M concentration in the electrolyte is presented in Figure 6b. A small diminution of peaks A2-A3and C1-C3 accompanies. In addition, two anodic peaks in the entire domain of the sweep of potential are observed. The appearance of an anodic peak in the anodic as well as in the reverse half cycles is the distinct feature of ethylene glycol electro-oxidation on noble metals in both acidic and alkaline solutions. So, it seems that methanol initially chemisorbs on the lower valence state oxides of copper and further oxidizes in higher overpotential [44]. Moreover, the peak due to ethylene glycol oxidation was reproducible with no evidence of film formation or electrode passivation.

The Cu(III) species that is generated at positive potentials has been reported to have the role of a redox mediator in the oxidation of several compounds at copper electrodes [45-46] and the electrode reaction may take place with a mechanism involving a rate limiting step where a reaction intermediate is formed upon a chemical reaction with a Cu(III) species. Fleischmann et al. [17,45] have postulated that the oxidation of amines and alcohols on nickel, copper, silver and cobalt oxide surfaces requires, in a first step, the stripping of a hydrogen atom from the substrate and that further reactions proceed through mechanisms involving the formation of free radicals. Marioli and Kuwana [47] have suggested a different route for the oxidation of carbohydrates on copper oxide since a remarkable diminution of Cu(II)oxide peak has been observed upon adding the substrate. It has been proposed that the carbohydrate interact (or complex) with Cu(I) diminishing the formation of Cu(II) and soluble species. Johnson and coworkers have proposed that the neutral hydroxide radical generated from the reaction of Cu(III) with hydroxide ion is the active species in the oxidation of carbohydrates.

In figure 6, according to the high current density in presence of ethylene glycol and also observation of a new oxidation peak for ethylene glycol oxidation at a potential much more negative than that of the generation of Cu(III), it have concluded that Cu(III) species have no effective role in ethylene glycol oxidation and therefore chemical oxidation mechanism through Cu(III) is not supporting the high oxidation current density in presence of ethylene glycol. We assume that anodic current is due to ethylene glycol oxidation on the surface of Cu(II)oxide layer by direct electro-oxidation.
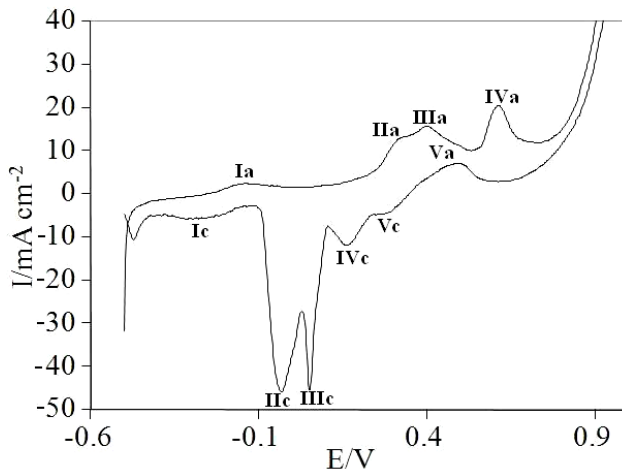
$$\text{Cu(II)oxide-ethylene glycol} \rightarrow$$
$$\text{Cu(II)oxide-intermediates} + e \quad (30)$$

Figure 7. First cyclic voltammograms at 20 mV s^{-1} of an Ag electrode in 0.1 M NaOH.

$$\text{Cu(II)oxide-intermediates} \rightarrow$$
$$\text{Cu(II)oxide-}\left[\left(COO^-\right)_2\right]_{ads} + e \quad (31)$$
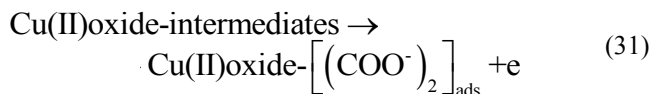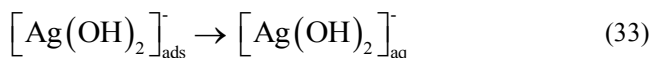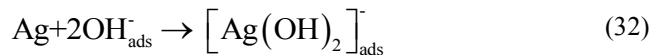
Figure 7 shows a typical first cyclic voltammetric scan of an Ag electrode in 0.1 M NaOH at 25 °C between -500 mV and 900mV at a scan rate of 20 mV s^{-1}. The anodic excursion span characterized by four anodic peaks (three major ones (IIa, IIa and IVa) and one minor (Ia)) prior to oxygen evolution potential. The reverse potential scan exhibits an activated anodic current peak (Va) and five cathodic contributions (Ic-Vc) prior to hydrogen evolution potential.

The first small anodic peak at -145 mV can be due to the under-potential silver oxidation and monolayer formation of Ag$_2$O or AgOH [48]. The second anodic peak at 330 mV could be attributed to the electrodissolution of Ag to [Ag(OH)$_2$]$^-$ through adsorption of OH$^-$ and desorption and diffusion of soluble [Ag(OH)$_2$]$^-$ [48-49]:

$$Ag + 2OH^-_{ads} \rightarrow \left[Ag\left(OH\right)_2\right]^-_{ads} \quad (32)$$

$$\left[Ag\left(OH\right)_2\right]^-_{ads} \rightarrow \left[Ag\left(OH\right)_2\right]^-_{aq} \quad (33)$$

The anodic peak, IIIa, can be ascribed to the thickening of the completed basal monolayer, i.e. the electroformation of a multi-layer of Ag$_2$O. It has been reported that the thickening process occurs via a 3D nucleation and growth mechanisms [50,51] according to

$$2Ag + 2OH^- \rightarrow Ag_2O + H_2O + 2e \quad (34)$$

Alternatively the appearance of two overlapped anodic peaks (IIa, IIIa) can be attributed to formation of different crystallographic form Ag$_2$O [52].

The anodic peak IVa is due to the electrooxidation of Ag$_2$O and the formation of AgO according to the overall electrochemical

A Comparative Study of the Electrooxidation of Ethylene Glycol on Transition Metal Electrodes in Alkaline Solution
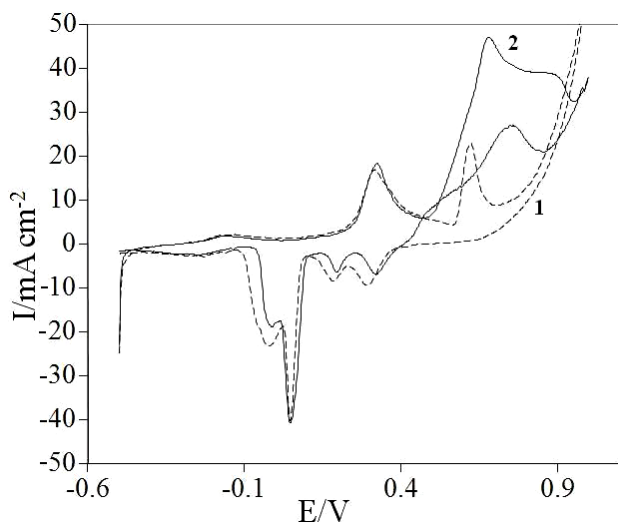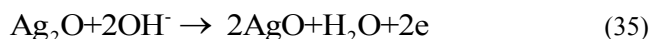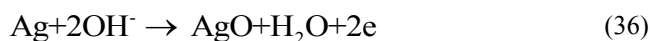*/ J. New Mat. Electrochem. Systems*

261

Figure 8. Cyclic voltammograms of silver electrode in 0.1 M NaOH solution in absence (1) and presence (2) of 0.2 M ethylene glycol at a scan rate of 20 mV s^{-1}.

reaction [47,53]

$$Ag_2O+2OH^- \rightarrow 2AgO+H_2O+2e \qquad (35)$$

In addition, it is possible that direct electrooxidation of Ag to AgO occurs within the potential range of peak IVa [54,55]:

$$Ag+2OH^- \rightarrow AgO+H_2O+2e \qquad (36)$$

The existence of anodic peak Va at the reveres scan in the potential range of 490 mV could be attributed to continuous nucleation and growth of an Ag$_2$O film as a result of electrooxidation of the Ag metal [53].

The small cathodic peak Vc at 270 mV might be related to the electroreduction of Ag$_2$O$_3$ to AgO which produced just prior to oxygen evolution potential [51,56].
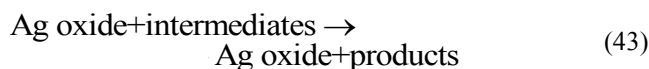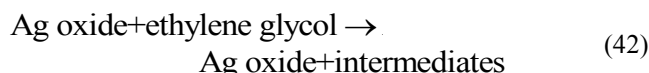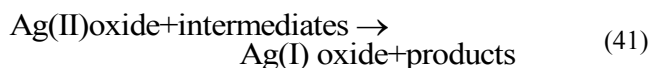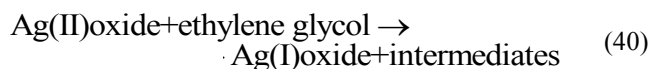
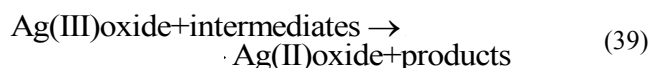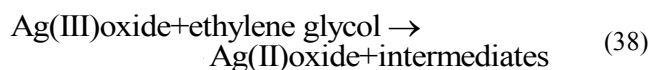$$2AgO+2OH^- \rightarrow Ag_2O_3+H_2O+2e \qquad (37)$$
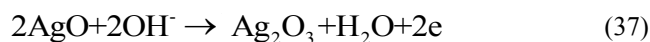
The cathodic peak IVc is ascribed to the electroreduction of AgO to Ag$_2$O according to reaction (35). On the other hand, the more negative cathodic peaks IIIc and IIc could be related to processes involved in electroreduction of Ag(I)oxide species. Its appearance indicates the complex nature of formed Ag$_2$O. Monolayer of underpotential Ag oxide is reduced in potential -250 mV in the end of voltammogram.

Fig. 8 shows second cyclic voltammograms of Ag electrode in 0.1 M NaOH solution and also voltammogram in the presence of 0.2 M ethylene glycol. In the second cycle variation is observed and in further cycle, voltamograms will be reproducible. In direct scan overlapping is occurred in second and third oxidation peaks and the peak current of Ag$_2$O$_3$ reduction is increased due to increased production in subsequent cycles.

In presence of ethylene glycol oxidation current increase at 500 mV is due to ethylene glycol oxidation. The CV in other regions remain the same as in the absence of ethylene glycol. Oxidation starts before AgO production and continues to 950 mV. The new oxidation peak observed in the anodic scan after AgO oxidation at 880 mV is attributed to the direct oxidation of ethylene glycol on the oxide surface. Therefore it is clear that multilayer Ag(II) and Ag(III)oxide, but not multilayer Ag(I) oxide, catalyzes the electrooxidation of ethylene glycol. It should also be noted that the peak potentials of all the peaks of both underpotential and multilayer Ag oxide formation and reduction were essentially unaffected by the presence of 0.5 M ethylene glycol, which indicates that there is no strong interaction of ethylene glycol with Ag. In the negative sweep ethylene glycol oxidation peak at 740 mV is observed due to the regeneration of active sites for adsorption of ethylene glycol as a result of the removal of adsorbed intermediates and products. In reverse scan decreasing charge is observed in the electroreduction of Ag(III) and Ag(II)oxide in potentials 310 and 185 mV. It seems that some Ag(III) and Ag(II)oxide is consumed in positive sweep in presence of ethylene glycol. Therefore indicating that ethylene glycol is oxidized already in the positive sweep by electrooxidation on Ag oxide layer and/or through chemical oxidation by the Ag(III) and Ag(II)oxide.

$$\begin{aligned} Ag(III)oxide+ethylene\ glycol \rightarrow \\ Ag(II)oxide+intermediates \end{aligned} \qquad (38)$$

$$\begin{aligned} Ag(III)oxide+intermediates \rightarrow \\ Ag(II)oxide+products \end{aligned} \qquad (39)$$

$$\begin{aligned} Ag(II)oxide+ethylene\ glycol \rightarrow \\ Ag(I)oxide+intermediates \end{aligned} \qquad (40)$$

$$\begin{aligned} Ag(II)oxide+intermediates \rightarrow \\ Ag(I)\ oxide+products \end{aligned} \qquad (41)$$

$$\begin{aligned} Ag\ oxide+ethylene\ glycol \rightarrow \\ Ag\ oxide+intermediates \end{aligned} \qquad (42)$$

$$\begin{aligned} Ag\ oxide+intermediates \rightarrow \\ Ag\ oxide+products \end{aligned} \qquad (43)$$

According to experimental results, anodic current density obtained from ethylene glycol oxidation on surface of oxide layer of metals has the order Ag>Cu>Ni>Pt>Au and Overpotential that was necessary for electrooxidation had the order Ag>Cu>Ni>Pt>Au.

The measurements of open circuit potentials as a function of immersion time are used to monitor some aspects of the chemical adsorption and electrocatalytic oxidation. The OCP curves of the Pt and Au electrode in NaOH solution without and containing ethylene glycol for 1500 s potentials measurements are shown in Fig. 9. As can be seen, the OCP increases suddenly to noble values and then approaches to steady state potential. The ennobling of the electrode potential in 0.1 M NaOH solution is due to healing and thickening of the oxide film carried by the metal surface. The reduction of oxygen is the only feasible process to account for the partial cathodic process of corrosion reaction. For currentless oxide film formation, it has been suggested [57] that the driving force of the surface oxide film formation on metal is the free energy change of the reaction between metal and solution. This reaction is as-
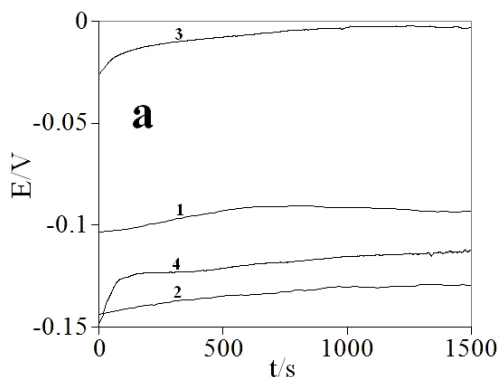
Figure 9. Variation in the open circuit potential in absence and presence of ethylene glycol, 1) Au, 2) Au-EG, 3) Pt.

sumed to proceed by migration of positive metal ion and/or oxygen ion vacancies from metal towards the electrolyte or possibly by migration of negative oxygen ion in opposite direction [57]. The fielding oxide film is assumed to decrease as the oxide thickness increases until a steady film thickness is reached, where a steady state potentials is attained.

In presence of ethylene glycol steady state potentials in solution tend towards more negative values. Figure 9 shows that in case of Pt and Au, a large potential variation was observed due to interaction with ethylene glycol according to the strong adsorption and oxidation in low potentials [58].

4. CONCLUSION

The oxide film of metals was formed electrochemically on surface of electrodes in a regime of cyclic voltammetry and tested for electro-oxidation of ethylene glycol in alkaline media. The metal electrodes showed activity for the oxidation of ethylene glycol in different potential range. Silver shows higher anodic current density for ethylene glycol oxidation and gold need lower overpotential in electrocatalytic oxidation. Ethylene glycol was oxidized on platinum electrode in different potential regions but on the other electrodes, oxidation was occurred in limited potential range. Ethylene glycol electrooxidation interfered with hydrogen adsorption/desorption on platinum and gold surface but on nickel and copper and silver electrode oxidation occurred near oxygen evolution. Open circuit potentials measurements indicate the strong adsorption of ethylene glycol on platinum and gold surface.

REFERENCES

[1] Y. Wang, L. Li, L. Hu, L. Zhuang, J. Lu, B. Xu, Electrochem. Commun., 5, 662 (2003).

[2] C.-C. Yang, Int. J. Hydrogen Energy, 29, 135 (2004).

[3] I. Danaee, M. Jafarian, A. Mirzapoor, F. Gobal, M.G. Mahjani, Electrochim. Acta, 55, 2093 (2010).

[4] B.I. Podlovchenko, O.A. Petry, A.N. Frumkin, H. Lal, J. Electronal. Chem., 11, 12 (1966).

[5] S. Rousseau, C. Coutanceau, C. Lamy, J.-M. Le´ger, J. Power Sources, 158, 18 (2006).

[6] T. Iwasita, E. Pastor, Electrochim. Acta, 39, 531, (1994).

[7] E. Peled, V. Livshits, T. Duvdevani, J. Power Sources, 106, 245 (2002).

[8] V. Livshits, E. Peled, J. Power Sources, 161, 1187 (2006).

[9] B. Wieland, J.P. Lancaster, C.S. Hoaglund, P. Holota, W.J. Tornquist, Langmuir, 12, 2594 (1996).

[10] C. Jin, Y. Song, Z. Chen, Electrochim. Acta, 54, 4136 (2009).

[11] Y.J. Fan, Z.Y. Zhou, C.H. Zhen, C.J. Fan, S.-G. Sun, Electrochim. Acta, 49, 4659 (2004).

[12] J.F.E. Gootzen, W. Visscher, J.A.R. Van Veen, Langmuir, 12, 5076 (1996).

[13] M.J. Gonzalez, C.T. Hable, M.S.Wrighton, J. Phys. Chem. B, 102, 9881 (1998).

[14] O.V. Cherstiouk, E.R. Savinova, L.A. Kozhanova, V.N. Parmon, React. Kinet. Catal. Lett., 69, 331 (2000).

[15] A. Dailey, J. Shin, C. Korzeniewski, Electrochim. Acta, 44, 1147 (1998).

[16] R.B. de Lima, V. Paganin, T. Iwasita, W. Vielstich, Electrochim. Acta, 49, 85 (2003).

[17] M. Fleischmann, K. Korinek, D. Pletcher, J. Electroanal. Chem., 31, 39 (1971).

[18] C. Y´a˜nez, C. Guti´errez, M.S. Ureta-Za˜nartu, J. Electroanal. Chem., 541, 39 (2003).

[19] M. Jafarian, F. Forouzandeh, I. Danaee, F. Gobal, M.G. Mahjani, J. Solid State Electrochem., 13, 1171 (2009).

[20] I. Danaee, M. Jafarian, F. Forouzandeh, F. Gobal, M.G. Mahjani, Electrochim. Acta, 53, 6602 (2008).

[21] J.-L. Boudenne, O. Cerclier, P. Bianco, J. Electrochem. Soc., 145, 2763 (1998).

[22] M. Gattrell, D.W. Kirk, J. Electrochem. Soc., 140, 1534 (1993).

[23] Y.F. Yang, G. Denuault, J. Electroanal. Chem., 443, 273 (1998).

[24] C.C. Hu, K.Y. Liu, Electrochim. Acta, 44, 2727 (1999).

[25] S. Hughes, P.L. Meschi, D.C. Johnson, Anal. Chim. Acta, 132, 1 (1981).

[26] E. Skou, Electrochim. Acta, 22, 313 (1977).

[27] L.E. Essis Yei, B. Beden, C. Lamy, J. Electroanal. Chem., 246, 349 (1988).

[28] C. Xu, R. Zeng, P.K. Shen, Z. Wei, Electrochim. Acta, 51, 1031 (2005).

[29] A.V. Tripkovic, K. Dj. Popovic, J.D. Momcilovic, D.M. Drazic, J. Electroanal. Chem., 448, 173 (1998).

[30] M.El M. Chbihi, D. Takky, F. Hahn, H. Huser, J.M. Leger, C. Lamy J. Electroanal. Chem., 463, 63 (1999).

[31] K. Matsuoka, Y. Iriyama, T. Abe, M. Matsuoka, Z. Ogumi, Electrochim. Acta, 51, 1085 (2005).

[32] Z. Borkowska, A. Tymosiak-Zielinska, G. Shul, Electrochim. Acta, 49, 1209 (2004).

[33] P. Parpot, P.R.B. Santos, A.P. Bettencourt, J. Electroanal. Chem., 610, 154 (2007).

[34] I. Danaee, M. Jafarian, F. Forouzandeh, F. Gobal, M.G. Mahjani, J. Phys. Chem. B 112, 15933 (2008).

A Comparative Study of the Electrooxidation of Ethylene Glycol on Transition Metal Electrodes in Alkaline Solution
/ J. New Mat. Electrochem. Systems

263

[35]I. Danaee, M. Jafarian, F. Forouzandeh, F. Gobal, M.G. Mahjani, Int. J. Hydrogen Energy, 33, 4367 (2008).

[36]I. Danaee, M. Jafarian, F. Forouzandeh, F. Gobal, M.G. Mahjani, Int. J. Hydrogen Energy 34, 859 (2009).

[37]J.M.M. Droog, C.A. Alderliesten, P.T. Alderliesten, G.A. Bootsma, J. Electroanal. Chem., 111, 61 (1980).

[38]J.M.M. Droog, B. Schlenter, J. Electroanal. Chem., 112, 387, (1980).

[39]C.H. Pyun, S.M. Park, J. Electrochem. Soc. 132, 2024 (1986).

[40]S.M. Abd El Haleem, B.G. Ateya, J. Electroanal. Chem. 117, 309 (1981).

[41]S.T. Farrell, C.B. Breslin, Electrochim. Acta, 49, 4497 (2004).

[42]A.M. Shams El Din, F.M. Abd El Wahab, Electrochim. Acta, 9, 113 (1964).

[43]B. Miller, J. Electrochem. Soc., 116, 1675 (1969).

[44]L.D. Burke, K.J. O'Dwyer, Electrochim. Acta, 36, 1937 (1991).

[45]M. Fleischmann, K. Korinek, D. Pletcher, J. Chem. Soc., Perkin Trans., 2, 1396 (1972).

[46]D. Meyerstein, F.M. Hawkridge, T. Kuwana, J. Electroanal. Chem., 40, 377 (1972).

[47]J.M. Marioli, T. Kuwana, Electrochim. Acta, 37, 1187 (1992).

[48]B.V. Tilak, R.S. Perkins, H.A. Kozlowska, B.E. Conway, Electrochim. Acta 17, 1447 (1972).

[49]J. Ambrose, R.G. Barradas, Electrochim. Acta, 19, 781 (1974).

[50]R.D. Giles, J.A. Harrison, J. Electroanal. Chem. 27, 161 (1970).

[51]G.T. Burstein, R.C. Newman, Electrochim. Acta, 25, 1009, (1980).

[52]R.F. Amlie, H.N. Honer, P. Ruetschi, J. Electrochem. Soc., 112, 1073 (1965).

[53]P. Stonehart, Electrochim. Acta, 13, 1789 (1968).

[54]M. Hepel, M. Tomkiewicz, C.L. Forest, J. Electrochem. Soc., 133, 468 (1986).

[55]R.C. Salvarezza, J.G. Becerra, A.J. Arvia, Electrochim. Acta, 33, 1753 (1988).

[56]N.A. Hampson, K.I. McDonald, J.B. Lee, J. Electroanal. Chem., 32, 165 (1971).

[57]A. M. Shams El Din, N.J. Paul, Thin Solid Films, 189, 205 (1990).

[58]E. Sitta, H. Varela, J. Solid State Electrochem., 12, 559 (2008).